*metals*

MDPI

*Editorial*

# Superconductivity 2022

**Michael Rudolf Koblischka * and Anjela Koblischka-Veneva**

Experimental Physics, Saarland University, P.O. Box 151150, D-66041 Saarbrücken, Germany; a.koblischka@gmail.com

* Correspondence: m.koblischka@gmail.com or m.koblischka@ieee.org

**Abstract:** Superconductivity in metals and alloys, i.e., conventional superconductivity, has seen many new developments in recent years, leading to a renewed interest in the principles of superconductivity and the search for new materials. The most striking discoveries include the near-room-temperature superconductivity in metal hydrides ($LaH_{10}$) under pressure, the extreme stability of superconductivity in NbTi up to 261 GPa pressure, the discovery of high-entropy alloy (HEA) superconductor materials, and the machine learning prediction of new superconducting materials. Other interesting research concerns the properties of 2D superconductors, topological superconductors, e.g., in hybrid systems, and the use of nanotechnology to create nanowires and nanostructures with new properties. Furthermore, and most importantly, the drive from new accelerator and fusion reactors for stronger superconducting magnets has lead to improved cable materials, showing the highest critical current densities ever. Thus, this Special Issue aims to bring together a collection of papers reflecting the present activity in this field.

**Keywords:** conventional superconductivity; high pressure; room-temperature superconductivity; metal hydrides; HEAs; Matthias rules; machine learning; 2D superconductors; topological superconductors; nanostructures; cables



**Citation:** Koblischka, M.R.; Koblischka-Veneva, A. Superconductivity 2022. *Metals* **2022**, *12*, 568. https://doi.org/10.3390/met12040568

Received: 23 March 2022
Accepted: 24 March 2022
Published: 28 March 2022



## 1. Introduction

Presently, 110 years after the discovery of superconductivity in the element Hg, research on superconductivity in metals and metallic alloys is again at the forefront of science with the discovery of (near) room-temperature superconductivity in $La(H_{10})$ hydrides, even if this is only at high pressures [1,2]. Very interestingly, the superconductivity in these metal hydrides is found to be of the conventional type, not involving an exotic mechanism [3,4].

Thus, there is a lot of interesting, ongoing research considering metallic materials and superconductivity, stimulated by the following ground-breaking developments: research on high-pressure conditions for superconducting elements, with the current record holder being Ca with a superconducting transition temperature, $T_c$, of 20 K or above [5]; the finding of the enormous stability of superconductivity at high pressures (261 GPa) of the otherwise well-known alloy NbTi, with an increased $T_c$ of up to 20 K [6]; many more details of various hydrogen–metal systems being superconductors at ambient conditions as well as at high pressures [7,8]; the engineering of various 2D superconducting materials [9]; topological superconductivity in metallic alloys and heterostructures [10,11]; the discovery of the superconducting high-entropy alloy (HEA) systems [12–14]; the finding of new metallic alloys using the old Matthias' rules [15] and by machine learning approaches [16,17]. Furthermore, methods of nanotechnology enable the stabilization of different crystal structures, which are otherwise only stable at high pressures, in nanostructured systems. An example of this approach is superconducting Ga with a much higher $T_c$, as reported previously—with Ga being a type-II superconductor [18]. The superconducting transition temperatures may be positively affected by nanostructuring, and topologic superconductivity may be found in, for example, hybrid semiconducting/superconducting systems, which again stimulates many new investigations, both experimental and theoretical. Last but not least, here it

must be mentioned that the superconducting performance of NbTi- and $Nb_3Sn$-based superconducting cables is presently higher than ever before [19–21]; this is because of the improved flux pinning properties and developed production schemes, driven by the demands of the large-scale applications of superconducting magnets in particle colliders and fusion reactors. Therefore, the research on metallic superconductors is far from being dead, as feared after the discovery of the high-$T_c$ superconductors. So, the intention of this Special Issue—"Superconductivity 2022"—is to bring together a complete collection of research works on the current "*hot*" topics in this field, demonstrating the advances that this field has seen in recent years.

## 2. Room-Temperature Superconductivity in $LaH_{10}$

Let us start with the most outstanding finding of (near) room-temperature superconductivity in the $LaH_{10}$ system under high pressure [1,2]. Figure 1a presents resistance $R(T)$ measurements during cooling/warming in zero applied field and in magnetic fields up to 9 T, at a pressure of ∼250 GPa [1]. The inset to (a) gives some more details on the superconducting transition, showing an additional step. In [1], the authors ascribe this step to inhomogeneities in the sample, which was also seen in other high-pressure experiments [22]. Here, it must be mentioned that the samples are only stable under high applied pressures, so such inhomogeneities are to be expected. Furthermore, the isotope effect as predicted by the BCS theory could be demonstrated when using deuterium ($D_2$) instead of $H_2$ in the experiments. The presence of deuterium in $LaD_{10}$ reduces the experimentally determined transition temperature, $T_c$, from 249 K to 180 K as shown in Figure 1b. Typically, all the high-pressure measurements published are resistance measurements, as it is much more straightforward to realize electric contacts to the sample in the high-pressure cell. However, as the most important property of superconductivity is the Meissner effect, which can only be measured magnetically, some criticism appeared [23]. To resolve this problem, a miniaturized diamond anvil cell was developed [24,25], so magnetic measurements of the Meissner effect at high pressures could be performed within a commercial SQUID magnetometer. All these data are currently under review and only published in preprint servers—a demonstration of the ongoing research in this very interesting research direction.

Driven by the prediction from early as 1935 that metallic hydrogen would be a room-temperature superconductor [26,27], the $LaH_{10}$ system is currently the closest possible approach to such a configuration using high—but still reasonable—pressures. These striking results triggered many additional works, both experimental and theoretical, discussing the stability [3] and classification [28] of such highly hydrogen-loaded phases in the various other metal hydride systems (e.g., Pd-H, Y-H, ..., etc.) known.

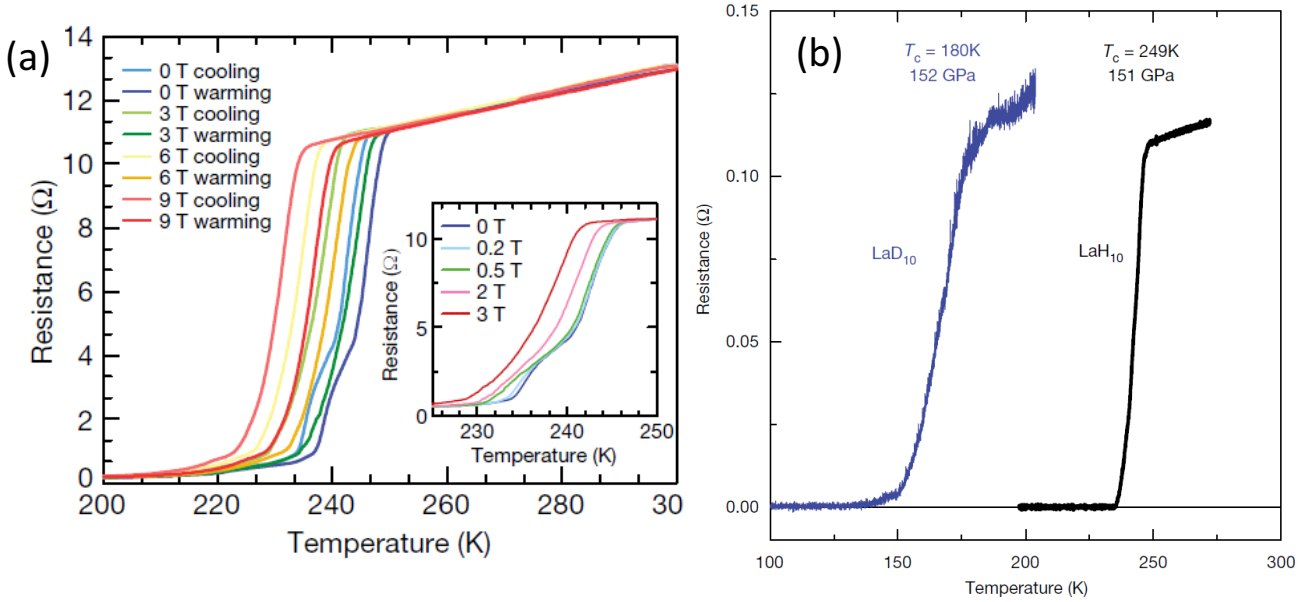


**Figure 1.** (Near) room-temperature superconductivity of $LaH_{10}$ [1]. (**a**) Resistance as function of temperature for the $LaH_{10}$ in applied magnetic fields up to 9 T. The width of the superconducting transition remains essentially constant up to 9 T. Both the cooling and the heating temperature sweeps are plotted, and $T_c$ was determined as the average of the two sweeps. An applied magnetic field of 9 T reduces the onset of the superconducting transition from around 250 K (as extracted from the heating curve) to around 240 K. The inset to (**a**) gives the superconducting transitions in more detail, revealing an additional step at zero field at ≈245 K. This step was found to disappear when applying a magnetic field of ∼3 T. The step was discussed in [1] to probably result from inhomogeneities in the superconducting sample, as has been seen in other high-pressure experiments, e.g., on a superconducting diamond doped with boron [22]. (**b**) Demonstration of the isotope effect in the $LaH_{10}$ system. The superconductive transition shifts to markedly lower temperatures after hydrogen is replaced by deuterium in samples with the same *fcc* crystal structure [1]. (**a**,**b**) Reprinted with permission from Ref. [1].

## 3. HEAs and High-Pressure Experiments on HEAs and NbTi

The next striking results must be presented in the order of time to better understand the developments made.

High-entropy alloys (HEAs) were discovered in 2004, which can be described as alloys or compounds that consist of several different types of randomly mixed constituent atoms and thus display a high degree of disorder, i.e., a high configurational entropy [29]. The HEA alloys exhibit fascinating properties, such as high yield strength and ductility, thermal stability, high strength at high temperatures, and strong resistance to corrosion and oxidation. The first report of superconductivity in such systems appeared after some time in 2014 by Koželj et al. [12] in the alloy $Ta_{34}Nb_{33}Hf_8Zr_{14}Ti_{11}$. This material shows a $T_c$ of 7.3 K and was characterized as a phonon-mediated type-II superconductor in the weak electron–phonon coupling limit.

The crystal structure of this first superconducting HEA was of the *bcc*-type (also called type-A HEA in Ref. [29]), as shown in Figure 2a. This was soon followed by other combinations of elements with the same crystal structure (e.g., NbTaTiZrSiGe and even one with Zr replaced by U), and then also different crystal structures were explored including the $\alpha$-Mn structure (e.g., $(ZrNb)_{0.1}(MoReRu)_{0.9}$, type-B HEA) and *hcp* structures (e.g., $Re_{0.56}Nb_{0.11}Ti_{0.11}Zr_{0.11}Hf_{0.11}$, type-D HEA) [13,14]. The developments in the field of superconducting HEAs were reviewed already by Sun and Cava [29] and Kitagawa, Hamamoto, and Ishizu [14]. Figures 2b,c show the A15 ($Cr_3Si$) structure of, e.g., $Nb_3Sn$. Two possible HEAs could be constructed: In (b), the chain site is only occupied by a single element, and all others share the second site, whereas in (c), all sites are shared among

all constituents. Following the nomenclature used by Sun and Cava [29], this would be a type-E HEA. An example of an A15-HEA is $(V_{0.5}Nb_{0.5})_{3-x}Mo_xAl_{0.5}Ga_{0.5}$ ($0.2 \leq x \leq 1.4$), showing superconductivity- and temperature-induced polymorphism. For $x$ =0.2, there are two polymorphs, one with the A15 structure ($T_c$ = 10.2 K, the other with *bcc* structure and not superconducting down to 1.8 K [30]. Figure 2d presents a HEA with an NaCl-type structure (type-C HEA), where the different metals occupy one (cationic) site in a shared fashion, and the other (anionic) site is only Te [31]. Remarkably, a superconducting HEA with an *fcc* structure had not yet been found.

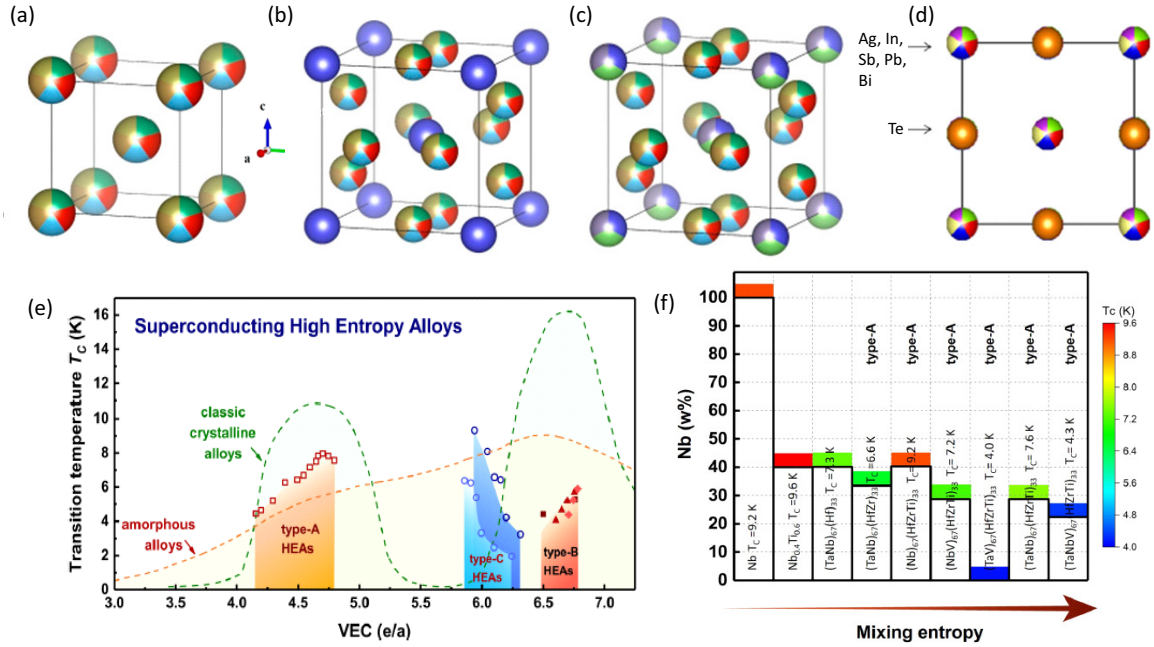


**Figure 2.** Possible crystal structures of HEAs: (**a**) body-centred cubic, (**b**) A15 structure ($Cr_3Si$-type) with HEA on the Si-site and (**c**) full A15 HEA. The multicoloured atoms indicate that the site is randomly occupied; solid lines represent the unit cells. Reprinted with permission from Ref. [14]. (**d**) presents a HEA with a cubic NaCl-type structure, where the different metals occupy one (cationic) site in a shared fashion, and the other (anionic) site is only Te. Reprinted with permission from Ref. [31]. (**e**) VEC dependence of $T_c$ for *bcc* HEA superconductors (data). The red-dashed ( - - - - - ) and green-dashed ( - - - - - ) lines give the VEC for crystalline 4d metal solution and amorphous 4D metal alloy superconductors, respectively. (**f**) shows the entropy effect in type-A HEAs compared to Nb and NbTi. (**e**,**f**) Reprinted with permission from Ref. [29].

An important tool to predict possible HEAs is the valence electron count (VEC). Maximum $T_c$ is reached at VEC ~4.7, which mimics the features of the Matthias rule for crystalline transition metal superconductors. Thus, the Matthias rules [32] again receive considerable interest among the researchers, not only for HEAs but also other types of alloys [15,33]. Considering the $T_c$-values of the type-A, type-B, and type-C HEA superconductors, a clear trend on the electron count can be observed. This is shown in Figure 3. The VEC dependence for the HEAs falls between those of crystalline 4D metal solid solutions as indicated using a dashed green line in Figure 2e and amorphous 4D alloys (dashed red line). The type-A (bcc) and type-C (CsCl-type) HEA superconductors with quite small unit cells seem to follow the two-peak character seen for the simpler binary alloys near VECs of 4.7 and 5.9, but not exactly. In contrast, the type-B HEAs with a more complex unit cell show a different behaviour. The following was stated in Ref. [29]: "It is a clear opportunity for future research to find an HEA superconducting system that is stable over a very wide range of VEC and study its superconducting properties". The preparation of HEA thin films will be especially interesting, for example, allowing the study of the flux pinning properties and the thickness dependence of $T_c$ in such HEA systems. As entropy

plays an important role in the definition of the HEA systems, it is still an open question how entropy affects superconductivity. From the data collected in Ref. [29], it looks that the entropy stabilizes the crystal structures, but does not play a role to determine the transition temperatures (see Figure 2f). Furthermore, to reach high $T_c$-values, the presence of Nb (the element with the highest $T_c$ at ambient pressure) seems to be crucial. Taking into account the fact that the alloy $Nb_{0.67}Ti_{0.33}$ is a superconductor showing $T_c = 9.2$ K, the atomic disorder introduced in the HEA has only a small influence on $T_c$.

In the view of possible applications of HEAs as new wire or cable materials, the *bcc* structure (space group $Im\bar{3}m$, No. 229) and the A15 structure (space group $Pm\bar{3}n$, No. 223) are the most interesting ones, where one could expect high critical current densities as well as high upper critical fields. However, up to now, the research had focused only on the preparation of phase-pure materials to best determine $T_c$, and not on the creation of possible flux pinning centres by varying the processing conditions or even adding secondary phases. Furthermore, the resulting microstructures have not yet been studied, including the character of the grain boundaries in polycrystalline materials. All this research will be a topic for future investigations.

The availability of the superconducting HEA material has triggered high-pressure experiments to learn more about the phase stability and the influence of high entropy under applied pressure. Thus, experiments were carried out on the *bcc* lattice HEA $(Nb,Ta)_{0.67}(Zr,Hf,Ti)_{0.33}$ material, with a $T_c$ of 7.8 K at ambient pressure, using diamond anvil cells, with the possibility to record data in applied magnetic fields as well as crystallographic information [34]. The results obtained are presented in Figure 3 and could be compared with existing data in the literature of the superconducting constituents Nb and Ta. The remarkable result obtained in these experiments is the demonstration of the outstanding stability of superconductivity in this HEA system—up to ~190 GPa—manifested by volume compression of 53% (190 GPa) and maintaining $T_c$ at about 9 K, and the upper critical field, $H_{c2}(0)$ at ~2 T, at this pressure. These observations unambiguously show that the electronic configuration of the HEA is clearly distinct from the elemental superconductors, Nb and Ta, contained in this HEA.

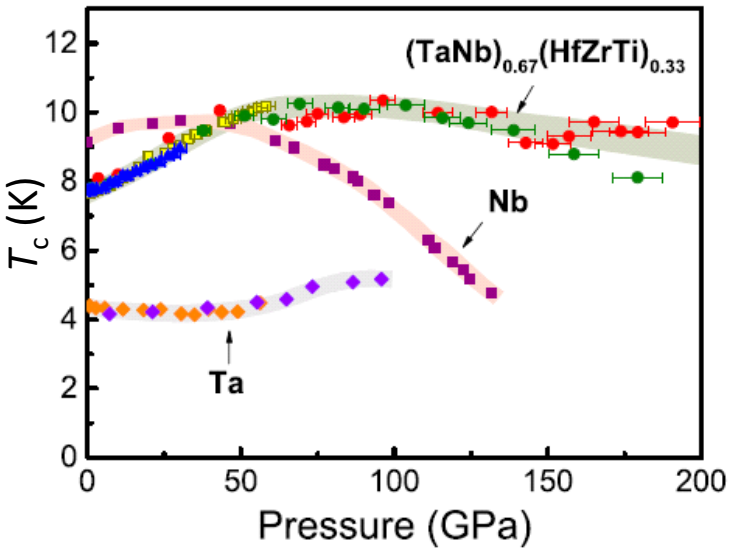


**Figure 3.** The pressure-dependent change of $T_c$ of the HEA and comparison with elemental Nb and Ta [34]. In this graph, $T_c$ for the HEA and the elemental Ta is defined as midpoint of the resistance transition curve (i.e., $T_c^{midpoint}$). $T_c$ of elemental Nb was determined by magnetic susceptibility measurements [35,36]. Solid circles (●, ●), blue triangles (▲), and yellow squares (■) are the data for the HEA obtained in [34]; the purple squares (■) and orange diamonds (♦) are data previously reported for elemental Nb [35,36]; and the violet diamonds (♦) are the data for elemental Ta [34]. Reprinted with permission from Ref. [34].

Another consequence of the high-pressure measurements on the HEA sample came the following year. It was realized that very many reports on NbTi exist in the literature since the 1960s, but no high-pressure measurement was ever performed in this system. Thus, Guo et al. [6] decided to apply high pressure to a commercially produced $Nb_{0.44}Ti_{0.56}$ alloy sample.

Again, the results obtained (see Figure 4) showed up with a striking result: The $T_c$ of NbTi could be raised from 9.6 K at ambient conditions up to 20 K under a pressure of 261 GPa, so NbTi remains superconducting even in the conditions of the outer core of Earth. Furthermore, the upper critical field, $H_{c2}$, increased from 15.4 K to 19 K at 1.8 K. These data set new record values for $T_c$ as well as for $H_{c2}$ of superconducting alloys consisting of only transition metal elements. Of course, these data provide not only record values for NbTi, but also enable new insights to the formation of the superconducting state in general.

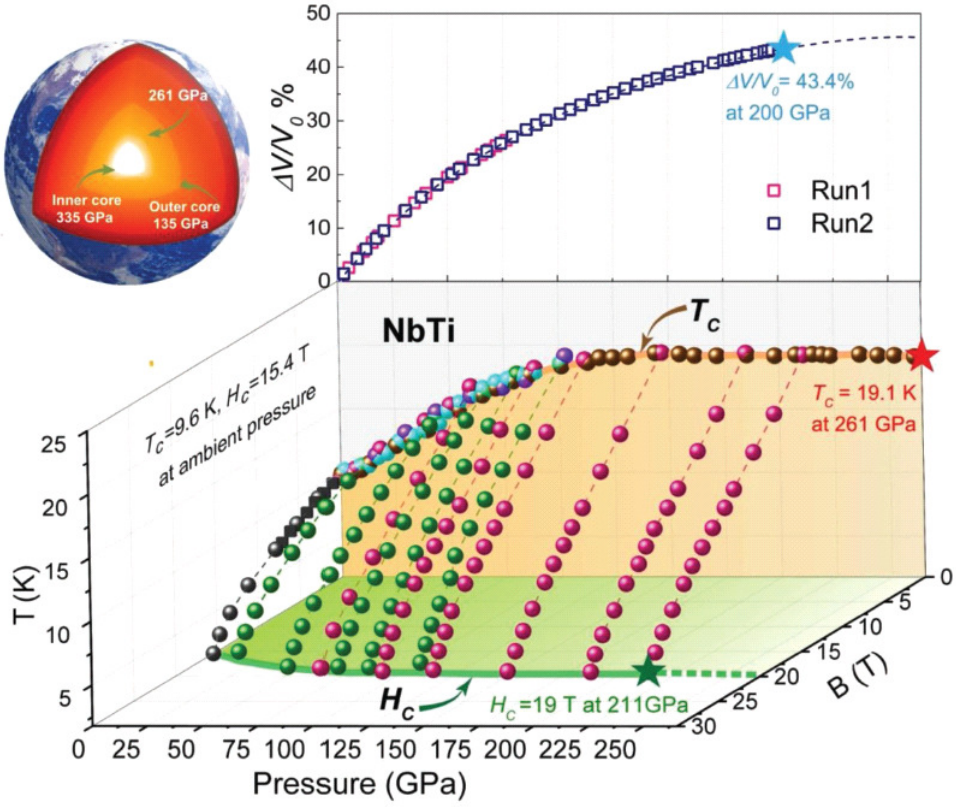


**Figure 4.** Superconductivity of the $Nb_{0.44}Ti_{0.56}$ alloy under various applied pressures and in various applied magnetic fields shown as a 3D plot of pressure (horizontal axis), temperature (vertical axis), and magnetic field. The solid orange line indicates the determined $T_c$ values (coloured balls represent $T_c$ obtained from different experimental runs), and the solid green line represents the behaviour of the upper critical field as function of temperature, $H_{c2}(T)$. The black, green, and red symbols (●, ●, ●) represent $T_c$ obtained in zero field and various applied magnetic fields. Furthermore, the pressure dependence of the molar volume is given as well ($-\Delta V = V_p - V_0$, where $V_p$ is the volume at fixed pressure and $V_0$ is the ambient pressure volume), the squares (□, □) represent the results obtained from the two independent runs. The red star (⋆) labels the $T_c$ value at 261 GPa, the green star (⋆) marks the upper critical field at $T = 1.8$ K, and the blue star (⋆) refers to the relative volume at the highest pressure investigated. The top left panel displays that the maximum pressure of this study falls in that of outer core of the earth. Reprinted with permission from Ref. [6].

## 4. Other Experiments

Besides these striking high-pressure results, there are also very interesting developments at ambient pressure. Besides the discovery of the HEA superconductors, other types of new alloys were found by applying the classic Matthias rules, e.g., in the system

LaBi [15], which demonstrates that still new materials can be found to be a superconductor. To find new superconductor materials, there is now the possibility to perform data searches using machine-learning-based algorithms, see, e.g., the reports in [16,17]. As the data of "classical" superconductors are well documented, there is a lot of information which can be used for searches of new material types. An important step forward will be the combination of the superconductor data ($T_c$, critical fields, critical currents) with crystallographic data. Exactly this task is fulfilled by the Roeser–Huber formalism, establishing a non-trivial relation between $T_c$ and the given crystal structures. For a successful application of the Roeser–Huber formalism, one needs the information of the possible crystal structures to determine the characteristic length, $x$, and about the electronic configuration (e.g., the VEC count, the ionic configuration) to count the number of charge carriers, $N_L$, and the number of passed (or near) atoms, $N_{\text{atoms}}$, as determined from the given crystal structure using the criterion $l/x < 0.5$ ($l$ is the distance of a given atom to the superconducting path in direction of $x$). The formalism was already applied to many superconducting material systems, but most importantly, for metals and alloys in Refs. [37–39]. The results obtained suggest the use of this approach in the machine learning algorithms to combine the crystallographic information with the superconductivity data.

Nanotechnology opened up new ways to fabricate materials in new shapes with approaches such as templating, laser cutting, FIB structuring, and more. Superconductivity in nanostructures may be completely different from the bulk counterparts. Recently, samples of nanostructured $\beta$-Ga wires were successfully prepared by a novel method of metallic flux nanonucleation within alumina oxide templates by Moura et al. [18] This enabled the determination of several superconducting parameters by means of magnetic measurements. The Ga nanowires were described as a weak-coupling type-II-like superconductor with a Ginzburg–Landau parameter $\kappa_{\text{GL}} = 1.18$, which is clearly favoured by the nanoscopic scale of the Ga nanowires. This result, including the measured relatively high $T_c$ of 6.2 K, is in stark contrast to pure bulk Ga, which is a type-I superconductor with a $T_c$ of only 1.8 K. This shows that phases, which are otherwise only stable at high pressures, may be stabilized as nanostructures. Thus, this opens up new ways to prepare superconducting materials with new properties.

As mentioned already in the introduction, the engineering of various 2D-superconducting materials with van der Waals (vdW)-coupled layers [9]—and of topological superconductivity in metallic alloys and heterostructures (e.g., superconducting/semiconducting) [10,11]—will continue to bring out interesting new developments. An remarkable example for this was presented recently in [40], showing the possibility of integrating superconducting, 2D-vdW $NbSe_2$ on paper to create paper-based, flexible electronics. This is shown in Figure 5.

Another material development similar to the HEAs is the so-called gummetal, which is a specific class of $\beta$-Ti alloys. After cold rolling, unusual mechanical behaviours, such as superelasticity and a low modulus, are obtained. Such materials are in practical use in wire frames for glasses or medical equipment including wires for orthodontic archwire brackets [14,41]. Gummetals are characterized by three factors all concerning the electronic configuration, which must be fulfilled at the same time. Among them is a VEC of 4.24 (see Figure 2e), so the electronic configuration may be quite similar to superconducting HEAs. First tests for superconductivity (AC susceptibility, resistance) on such an alloy (as-cast $Al_5Nb_{24}Ti_{40}V_5Zr_{26}$), which was recently reported to be a gummetal-like HEA alloy in [42] were carried out, showing superconductivity below 5 K [14]. Thus, one may hope that superconducting gummetals may be an excellent material for superconducting wires/cables or magnets, enabling a small bending radius while maintaining strong superconductivity.

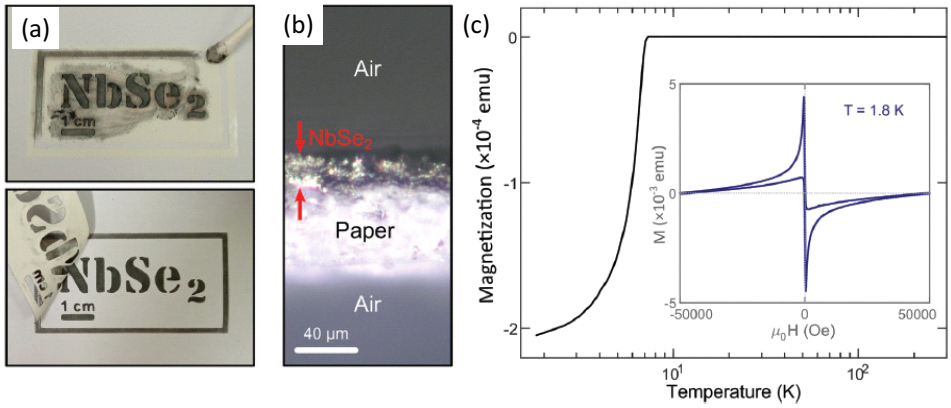


**Figure 5.** (**a**) Deposition of a $NbSe_2$ film on standard copy paper. The images were acquired during the deposition process of a $NbSe_2$ film on paper following an user-defined pattern using a vinyl stencil mask. (**b**) Optical microscopy image of a cross-section of the paper coated with a $NbSe_2$ film allowing an estimation of the $NbSe_2$ film thickness. (**c**) Magnetization vs. temperature measured after a zero-field cooling in 10 Oe applied magnetic field of $NbSe_2$ film on standard copy paper. Reprinted with permission from Ref. [40].

## 5. Summary

The most recent and striking results in the field of conventional superconductivity in recent years are summarized in this Special Issue. Based on these results, several directions for new research (high-pressure experiments, HEAs, nanostructured superconductors, gummetal) were outlined, thus demonstrating the large number of possible new activities in this field.

**Author Contributions:** Conceptualization, A.K.-V. and M.R.K.; formal analysis, A.K.-V. and M.R.K.; investigation, A.K.-V. and M.R.K.; visualization, A.K.-V. and M.R.K.; writing—original draft preparation, M.R.K.; writing—review and editing, A.K.-V. and M.R.K. All authors have read and agreed to the published version of the manuscript.

**Funding:** This work is part of the SUPERFOAM international project funded by ANR and DFG under the references ANR-17-CE05-0030 and DFG-ANR Ko2323-10, respectively.

**Institutional Review Board Statement:** Not applicable.

**Informed Consent Statement:** Not applicable.

**Data Availability Statement:** Not applicable.

**Conflicts of Interest:** The authors declare no conflict of interest.

## References

1. Drozdov, A.P.; Kong, P.P.; Minkov, V.S.; Besedin, S.P.; Kuzovnikov, M.A.; Mozaffari, S.; Balicas, L.; Balakirev, F.F.; Graf, D.E.; Prakapenka, V.B.; et al. Superconductivity at 250 K in lanthanum hydride under high pressures. *Nature* **2019**, *569*, 528–531. [CrossRef] [PubMed]
2. Somayazulu, M.; Ahart, M.; Mishra, A.K.; Geballe, Z.M.; Baldini, M.; Meng, Y.; Struzhkin, V.V.; Hemley, R.J. Evidence for Superconductivity above 260 K in Lanthanum Superhydride at Megabar Pressures. *Phys. Rev. Lett.* **2019**, *122*, 027001. [CrossRef]
3. Semenok, D.V.; Kruglov, I.A.; Savkin, I.A.; Kvashnin, A.G.; Oganov, A.R. On Distribution of Superconductivity in Metal Hydrides. *Curr. Opin. Solid State Mater. Sci.* **2020**, *24*, 100808. [CrossRef]
4. Kruglov, I.A.; Semenok, D.V.; Song, H.; Szczęśniak, R.; Wron, I.A.; Akashi, R.; Mahdi Davari Esfahani, M.; Duan, D.; Cui, T.; Kvashnin, A.G.; et al. Superconductivity of $LaH_{10}$ and $LaH_{16}$ polyhydrides. *Phys. Rev. B* **2020**, *101*, 024508. [CrossRef]
5. Yabuuchi, T.; Matsuoka, T.; Nakamoto, Y.; Shimizu, K. Superconductivity of Ca Exceeding 25 K at Megabar Pressures. *J. Phys. Soc. Jpn.* **2006**, *75*, 083703. [CrossRef]
6. Guo, J.; Lin, G.; Cai, S.; Xi, C.; Zhang, C.; Sun, W.; Wang, Q.; Yang, K.; Li, A.; Wu, Q.; et al. Record-High Superconductivity in Niobium–Titanium Alloy. *Adv. Mater.* **2019**, *31*, 1807240. [CrossRef] [PubMed]
7. Durajski, A.P.; Wang, C.; Li, Y.; Szczęśniak, R.; Cho, J.-H. Evidence of Phonon-Mediated Superconductivity in $LaH_{10}$ at High Pressure. *Ann. Phys.* **2021**, *533*, 2000518. [CrossRef]

8. Kostrzewa, M.; Szczęśniak, K.M.; Durajski, A.P.; Szczęśniak, R. From $LaH_{10}$ to room–temperature superconductors. *Sci. Rep.* **2020** *10*, 1592. [CrossRef]
9. Qiu, D.; Gong, C.; Wang, S.; Zhang, M.; Yang, C.; Wang, X.; Xiong, J. Recent Advances in 2D Superconductors. *Adv. Mater.* **2021**, *33*, 2006124. [CrossRef] [PubMed]
10. Sato, M.; Ando, J. Topological superconductors: A review. *Rep. Prog. Phys.* **2017**, *80*, 076501. [CrossRef]
11. Frolov, S.M.; Manfra, M.J.; Sau, J.D. Topological superconductivity in hybrid devices. *Nat. Phys.* **2020**, *16*, 718–724. [CrossRef]
12. Koželj, P.; Vrtnik, S.; Jelen, A.; Jazbec, S.; Jagličić, Z.; Saiti, S.; Feuerbacher, M.; Steurer, W.; Dolinšek, J. Discovery of a Superconducting High-Entropy Alloy. *Phys. Rev. Lett.* **2014**, *113*, 107001. [CrossRef]
13. Marik, S.; Motla, K.; Varghese, M.; Sajilesh, K.P.; Singh, D.; Breard, Y.; Boullay, P.; Singh, R.P. Superconductivity in a new hexagonal high-entropy alloy. *Phys. Rev. Mater.* **2019**, *3*, 060602(R). [CrossRef]
14. Kitagawa, J.; Hamamoto, S.; Ishizu, N. Cutting Edge of High-Entropy Alloy Superconductors from the Perspective of Materials Research. *Metals* **2020**, *10*, 1078. [CrossRef]
15. Kinjo, T.; Kajino, S.; Nishio, T.; Kawashima, K.; Yanagi, Y.; Hase, I.; Yanagisawa, T.; Ishida, S.; Kito, H.; Takeshita, N.; et al. Superconductivity in $LaBi_3$ with $AuCu_3$-type structure. *Supercond. Sci. Technol.* **2016**, *29*, 03LT02. [CrossRef]
16. Stanev, V.; Oses, C.; Kusne, A.G.; Rodriguez, E.; Paglione, J.; Curtarolo, S.; Takeuchi, I. Machine learning modeling of superconducting critical temperature. *NPJ Comput. Mater.* **2018**, *4*, 29. [CrossRef]
17. Konno, T.; Kurokawa, H.; Nabeshima, F.; Sakishita, Y.; Ogawa, R.; Hosako, I.; Maeda, A. Deep learning model for finding new superconductors. *Phys. Rev. B* **2021**, *103*, 014509. [CrossRef]
18. Moura, K.O.; Pirota, K.R.; Béron, F.; Jesus, C.B.R.; Rosa, P.F.S.; Tobia, D.; Pagliuso, P.G.; de Lima, O.F. Superconducting Properties in Arrays of Nanostructured $\beta$-Gallium. *Sci. Rep.* **2017**, *7*, 15306. [CrossRef]
19. Anvar, V.A.J.; Qin, Y.; Wu, T.; Bagni, A.; Devred, T.J.; Haugan, M.S.A.; Hossain, C.; Zhou, A. Nijhuis AC loss and contact resistance of different CICC cable patterns: Experiments and numerical modeling. *Fusion Eng. Des.* **2020**, *161*, 111898. [CrossRef]
20. Xu, X. A review and prospects for $Nb_3Sn$ superconductor development. *Supercond. Sci. Technol.* **2017**, *30*, 093001. [CrossRef]
21. Mitchell, N.; Breschi, M.; Tronza, V. The use of $Nb_3Sn$ in fusion: lessons learned from the ITER production including options for management of performance degradation. *Supercond. Sci. Technol.* **2020**, *33*, 054007. [CrossRef]
22. Zhang, G.; Samuely, T.; Kačmarčík, J.; Ekimov, E.A.; Li, J.; Vanacken, J.; Szabó, P.; Huang, J.; Pereira, P.J.; Cerbu, D.; et al. Bosonic anomalies in boron-doped polycrystalline diamond. *Phys. Rev. Appl.* **2016**, *6*, 064011. [CrossRef]
23. Hirsch, J.E.; Marsiglio, F. Clear evidence against superconductivity in hydrides under high pressure. *arXiv* **2022**, arXiv:2110.07568.
24. Minkov, V.S.; Bud'ko, S.; Balakirev, F.; Prakapenka, V.; Chariton, S.; Husband, R.; Liermann, H.-P.; Eremets, M.I. The Meissner Effect in High-Temperature Hydrogen-Rich Superconductors under High Pressure. Preprint, Researchsquare. Available online: https://www.researchsquare.com/article/rs-936317/v1 (accessed on 20 March 2022).
25. Eremets, M.I.; Minkov, V.S.; Drozdov, A.P.; Kong, P.P.; Ksenofontov, V.; Shylin, S.I.; Bud'ko, S.L.; Prozorov, R.; Balakirev, F.F.; Sun, D.; et al. High-Temperature Superconductivity in Hydrides: Experimental Evidence and Details. *arXiv* **2022**, arXiv:2201.05137.
26. Wigner, E.; Huntington, H.B. On the possibility of a metallic modification of hydrogen. *J. Chem. Phys.* **1935**, *3*, 764–770. [CrossRef]
27. Gregoryanz, E.; Ji, C.; Simpson, P.D.; Li, B.; Howie, R.T.; Mao, H.-K. Everything you always wanted to know about metallic hydrogen but were afraid to ask. *Matter Radiat. Extrem.* **2020**, *5*, 038101. [CrossRef]
28. Talantsev, E.F. Classifying hydrogen-rich superconductors. *Mat. Res. Expr.* **2019**, *6*, 106002. [CrossRef]
29. Sun, L.; Cava, R.J. High-entropy alloy superconductors: Status, opportunities, and challenges. *Phys. Rev. Mater.* **2019**, *3*, 090301. [CrossRef]
30. Jifeng Wu, J.; Liu, B.; Cui, Y.; Zhu, Q.; Xiao, G.; Wang, H.; Wu, S.; Cao, G.; Ren, Z. Polymorphism and superconductivity in the V-Nb-Mo-Al-Ga high-entropy alloys. *Sci. China Mater.* **2020**, *63*, 823–831. [CrossRef]
31. Mizuguchi, Y. Superconductivity in High-Entropy-Alloy Telluride $AgInSnPbBiTe_5$. *J. Phys. Soc. Jpn.* **2019**, *88*, 124708. [CrossRef]
32. Matthias, B.T.; Geballe, T.H.; Compton, V.B. Superconductivity. *Rev. Mod. Phys.* **1963**, *35*, 1. [CrossRef]
33. Conder, K. A second life of the Matthias' rules. *Supercond. Sci. Technol.* **2016**, *29*, 080502. [CrossRef]
34. Guo, J.; Wang, H.; von Rohr, F.; Wang, Z.; Cai, S.; Zhou, Y.; Yang, K.; Li, A.; Jiang, S.; Wu, Q.; et al. Robust zero resistance in a superconducting high-entropy alloy at pressures up to 190 GPa. *Proc. Nat. Acad. Sci. USA* **2017**, *114*, 13144–13147. [CrossRef]
35. Struzhkin, V.V.; Timofeev, Y.A.; Hemley, R.J.; Mao, H.K. Superconducting $T_c$ and electron-phonon coupling in Nb to 132 GPa: Magnetic susceptibility at megabar pressures. *Phys. Rev. Lett.* **1997**, *79*, 4262–4265. [CrossRef]
36. Tonkov, E.Y.; Ponyatovsky, E. *Phase Transformations of Elements Under High Pressure*; CRC Press LLC: Boca Raton, FL, USA, 2004; pp. 237–239.
37. Roeser, H.P.; Haslam, D.T.; Lopez, J.S.; Stepper, M.; von Schoenermark, M.F.; Huber, F.M.; Nikoghosyan, A.S. Correlation between transition temperature and crystal structure of niobium, vanadium, tantalum and mercury superconductors. *Acta Astronaut.* **2010**, *67*, 1333–1336. [CrossRef]
38. Koblischka, M.R.; Roth, S.; Koblischka-Veneva, A.; Karwoth, T.; Wiederhold, A.; Zeng, X.L.; Fasoulas, S.; Murakami, M. Relation between Crystal Structure and Transition Temperature of Superconducting Metals and Alloys. *Metals* **2020**, *10*, 158. [CrossRef]
39. Koblischka, M.R.; Koblischka-Veneva, A. Calculation of $T_c$ of Superconducting Elements with the Roeser–Huber Formalism. *Metals* **2022**, *12*, 337. [CrossRef]

40. Azpeitia, J.; Frisenda, R.; Lee, M.; Bouwmeester, D.; Zhang, W.; Mompean, F.; van der Zant, H.S.J.; García-Hernández, M.; Castellanos-Gomez, A. Integrating superconducting van der Waals materials on paper substrate. *Mater. Adv.* **2021**, *2*, 3274. [CrossRef] [PubMed]
41. Saito, T.; Furuta, T.; Hwang, J.-H.; Kuramoto, S.; Nishino, K.; Suzuki, N.; Chen, R.; Yamada, A.; Ito, K.; Seno, Y.; et al. Multifunctional Alloys Obtained via a Dislocation-Free Plastic Deformation Mechanism. *Science* **2019**, *300*, 464. [CrossRef] [PubMed]
42. Zherebtsov, S.; Yurchenko, N.; Panina, E.; Tikhonovsky, M.; Stepanov, N. Gum-like mechanical behavior of a partially ordered $Al_5Nb_{24}Ti_{40}V_5Zr_{26}$ high entropy alloy. *Intermetallics* **2020**, *116*, 106652. [CrossRef]